

ARMY RESEARCH LABORATORY



An Amplified Broadband Dipole E-Dot Sensor

by Christian G. Reiff

ARL-TR-1613

March 1998

DTIC QUALITY INSPECTED 2

19980325 048

Approved for public release; distribution unlimited.

The findings in this report are not to be construed as an official Department of the Army position unless so designated by other authorized documents.

Citation of manufacturer's or trade names does not constitute an official endorsement or approval of the use thereof.

Destroy this report when it is no longer needed. Do not return it to the originator.

Army Research Laboratory

Adelphi, MD 20783-1197

ARL-TR-1613

March 1998

An Amplified Broadband Dipole E-Dot Sensor

Christian G. Reiff

Sensors and Electron Devices Directorate

Approved for public release; distribution unlimited.

Abstract

This report describes the incorporation of an amplifier in a dipole sensor. The entire package is contained in a semirigid coaxial cable end. This configuration provides a flat E-dot field response from dc to 2 GHz. The amplification of the sensor response before cable losses allows the correction for the losses by convolution in the frequency domain. The MATLAB algorithms used to correct measurement system losses are described.

Contents

1. Introduction	1
2. Making the Sensor	1
3. Transfer Function	2
4. The Experiment	4
5. Results	9
6. Conclusions	13
References	15
Distribution	33
Report Documentation Page	35

Appendices

A.—MATLAB Function CALSTEP	17
B.—MATLAB Function CAL	23
C.—Data Correction Algorithm	27

Figures

1. Diagram of fabricated dipole sensor	2
2. Raw and corrected data for sensor	4
3. Simplified side view of G-TEM EMCO model 5317	5
4. TDR measurements of G-TEM cell	6
5. Measurements of applied electric fields	7
6. Transfer function magnitudes of 10× and 5× sensor amplifiers	7
7. Fields calculated from measured dipole voltage compared with 245-V G-TEM field at measurement location	9
8. Fields calculated from measured dipole voltage compared with 155-V G-TEM field at measurement location	10
9. Fields calculated from measured dipole voltage compared with 60-V G-TEM field at measurement location	10
10. Sensor response	12
11. Results of E-dot data with common mode noise removed	12
12. Transfer functions for three sensors used in experiment	14

1. Introduction

The accurate measurement of broadband pulse transients requires compensation for effects caused by measurement system characteristics. Components of a measurement system have different frequency characteristics. Simple components such as cables cause high-frequency rolloff. More complicated components such as amplifiers, sensors, and antennas have more complicated frequency characteristics. From measurements made on the measurement system, a transfer function is created that contains the information needed to compensate for the measurement system characteristics. This transfer function is deconvolved with a measured signal in the frequency domain to produce an accurate measurement representation.

Because the compensation is performed in the frequency domain, a small measured transient may have portions of its frequency content decreased below the noise floor by measurement system attenuation. A portion of the information to correct the measured signal has been lost, and when the transfer function is deconvolved with the measured signal, the noise replacing the lost information is being corrected, along with the remaining content of the measured signal.

An inexpensive solution to this problem is to amplify the signal at the sensor before most of the measurement system attenuation takes place. In this report, the process of placing an amplifier at a dipole junction is described. The measurements and calculations to determine the system transfer function and the application of the transfer function to the measured signal are described. Finally, an electric field is measured, corrected, and compared to the known field of a gigahertz-transverse electromagnetic (G-TEM) cell. This process is performed for three identically fabricated sensors with 10×, 5×, and no amplification included. The sensors produced accurate time-domain electric field measurements with factors of eight and five increased sensitivity compared to the nonamplified sensor from dc to 2 GHz.

2. Making the Sensor

The sensor is a dipole created at the end of a 1/8-in.-diameter solid copper shield coaxial cable (coax), which is used to support the dipole and provide a return path for the signal. The coax center conductor is one leg of the dipole, and the shield is the other leg. An amplifier is placed inside the coax outer conductor at the end of the coax. Pin sockets are used to facilitate the changing of dipole height without subjecting the amplifier to further soldering.

The Mini Circuits ERA-4 and ERA-5 amplifiers were used in this experiment. The small size, incorporated bias-T, and four-pin configuration made the amplifier ideal for this experiment. A great variety of amplifiers exist that could be used for this purpose with modifications in specifica-

tions or configuration. The four pins on the amplifier are input, output, and two grounds. A low-temperature soldering iron was used to solder the output pin to the center conductor of the coax. A short piece of coax shield was slotted at one end to fit over the ground pins of the amplifier. Small pin sockets were soldered to the other end of the slotted shield and to the input pin of the amplifier. The slotted shield was then soldered to the end of the coax and the slots were soldered to the ground pins, with care taken not to overheat the amplifier leads. The empty coax was then filled to the end with epoxy to support the amplifier and sockets. This process is illustrated in figure 1. Wires of the proper size to fit in the sockets are bent and trimmed to form the dipole legs in the size desired.

For the electric field to be proportional to the integral of the measured voltage measurement, the dipole dimension should be less than 1/10 of the shortest wavelength. The highest frequency expected is approximately 0.35 divided by the risetime. If the amplifier is within 1/10 wavelength of the end of the dipole at the highest frequency, there is no need to worry about impedance mismatches, because the physical configuration has negligible voltage change across its length.

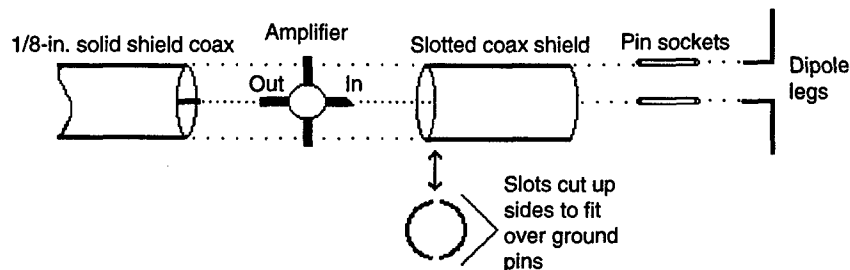
3. Transfer Function

A transfer function of a measurement system component is performed in the time domain by the application of a broadband transient and the measurement of the component effects on that transient. A step waveform produced by the Tektronix S-52 time-domain reflectometry (TDR) pulse generator is used as the applied waveform, because the 25-ps risetime provides ample high-frequency content, and the low-frequency content is determined by the measurement window. To establish a baseline of the applied signal with minimal perturbation, the pulse is measured through a 4-in. coax. A measurement through the full system cabling without the sensor establishes the system characteristics. The complete FFT technique [1] is used to provide a frequency-domain representation of the step pulse. The frequency-domain representations of the system measurement and the baseline measurement are now deconvolved with the use of an iterative method [2].

The frequency domain relation between a signal measurement and the actual signal measured is

$$Y(j\omega) = X(j\omega) \cdot H(j\omega), \quad (1)$$

Figure 1. Diagram of fabricated dipole sensor. (When all pieces have been soldered, the space around the amplifier is filled with epoxy.)



where $Y(j\omega)$ is the actual signal to be measured or the input to the measurement system component, $X(j\omega)$ is the measured signal data after the measurement system component or the output of the component, and $H(j\omega)$ is the transfer function of the measurement system component or a representation of the frequency-domain characteristics of the component. Values for Y and X are found in the time domain by measurement of the applied signal as accurately as possible and by measurement of the same applied signal through the measurement system component. To find the transfer function, one converts the Y and X data to the frequency domain and uses these to solve for $H(j\omega)$ using the optimal deconvolution expression [2]:

$$H(j\omega) = \frac{Y(j\omega) \cdot X^*(j\omega)}{|X(j\omega)|^2 + \lambda}, \quad (2)$$

where λ is the optimization parameter to be varied in the iteration process, and $*$ denotes the complex conjugate.

The preceding process to find a transfer function, given baseline and component time domain data sets, was implemented in a MATLAB function CALSTEP, shown in appendix A. To comply with local tradition, we solve for $1/H(j\omega)$, or output over input. The process is the same, with X and Y variables exchanged. Progress toward a solution is determined with the use of a graphic interface and knowledge of the frequency content of the applied waveform. A value of zero for λ will result in a simple division of $X(j\omega)$ by $Y(j\omega)$ to find $1/H(j\omega)$, which is very noisy when $Y(j\omega)$ is small and $X(j\omega)$ is not, as in noisy regions. When λ is zero, all information in the measured data is present, including the noise. As λ is increased, a filtering effect occurs when $Y(j\omega)$ is very small. This filtering occurs in the high frequencies, where the magnitudes are very small for our pulse-type waveform.

The graphic representation that is used to determine progress plots the transfer function for λ equal to zero and the present iterative value of λ . The plot is windowed vertically to increase the sensitivity to the divergence of the curves. A vertical dotted line is drawn at the high-frequency limit of the applied signal. The deconvolution is considered optimum when the curves overlay to the high-frequency limit. Beyond that point is only information on noise, which can be filtered. For signals with poles and zeros, the curves should overlay, except at the minimums.

A transfer function can be made for the system from the scope to the sensor if the attenuation is small enough. If it is necessary to create transfer functions for individual components, they can be combined into a total transfer function through multiplication. The differences between single and combined transfer functions are negligible. The scope is assumed to have no frequency characteristics. A sensor usually has to be calibrated separately.

The transfer function for the measurement system is applied to a measured signal with the use of the MATLAB function CAL, which is shown

in appendix B. This function uses the previously calculated transfer function and the measured time-domain signal as input. The time-domain signal is converted to the frequency domain, and the result is deconvolved with the same method used to create the transfer function. The transfer function being $1/H(j\omega)$ allows the use of the same calculation. The result is converted to the time domain with an inverse fast Fourier transform (FFT). The result of this process is shown in figure 2. This corrected waveform is then integrated and processed to produce the electric field transient.

4. The Experiment

The surest way to determine the quality of electric field measurements provided by the amplifier/dipole combination is to measure a known field. Our G-TEM cell (EMCO model 5317) provides a known field to within ± 5 dB when using a continuous wave (cw) source above 1 GHz [3]. The uncertainty is due to standing waves caused by reflection from the absorber. In the time domain, however, a narrow pulse could be measured before the reflections arrive. A side view of the G-TEM cell is shown in figure 3. The G-TEM cell is an enclosed chamber, shaped like a horn antenna with a horizontal center plane or septum. This creates a transmission line of constant impedance and increasing volume. The large end of the chamber is enclosed, and the wall is covered with electromagnetic absorbing material. The source voltage is applied at the small end of the chamber between the septum and the chamber shell. The G-TEM electric field at a point in the cell could be determined from the applied voltage and the height of the septum if there are no discontinuities before that point. The field would follow a curve to remain perpendicular to the conductive surfaces of the G-TEM cell. Rough measurements to find the divergence angle at the measurement location indicate that 99 percent of the electric field is vertical.

Figure 2. Raw and corrected data for sensor with (a) ground leg down and (b) ground leg up. Data has measurement system frequency domain characteristics removed (i.e., cable, delay line, and amplifier characteristics).

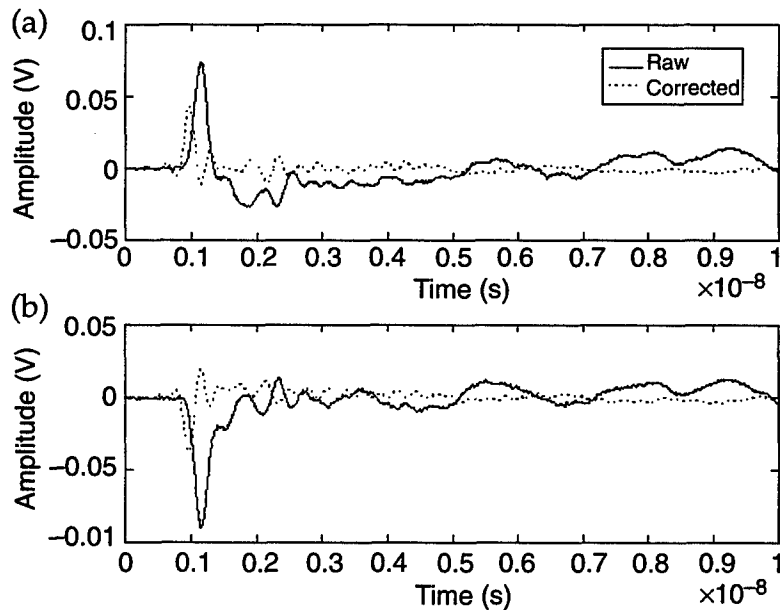
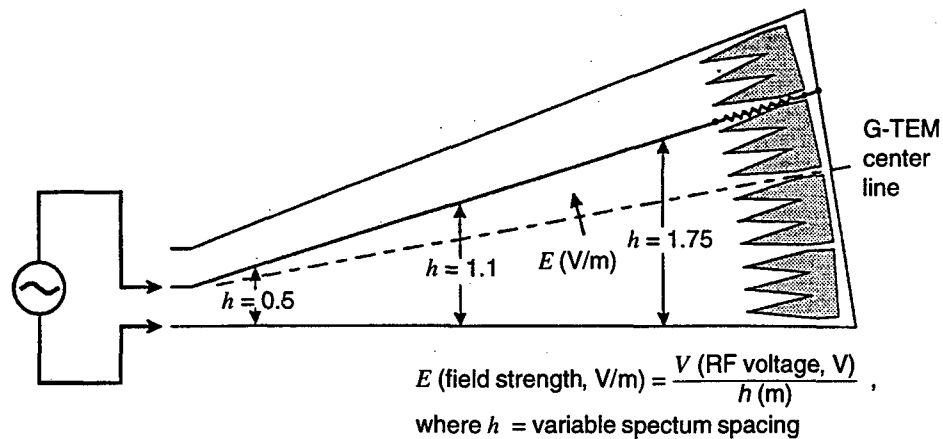


Figure 3. Simplified side view of G-TEM EMCO model 5317 showing physical placement of septum and cell walls.

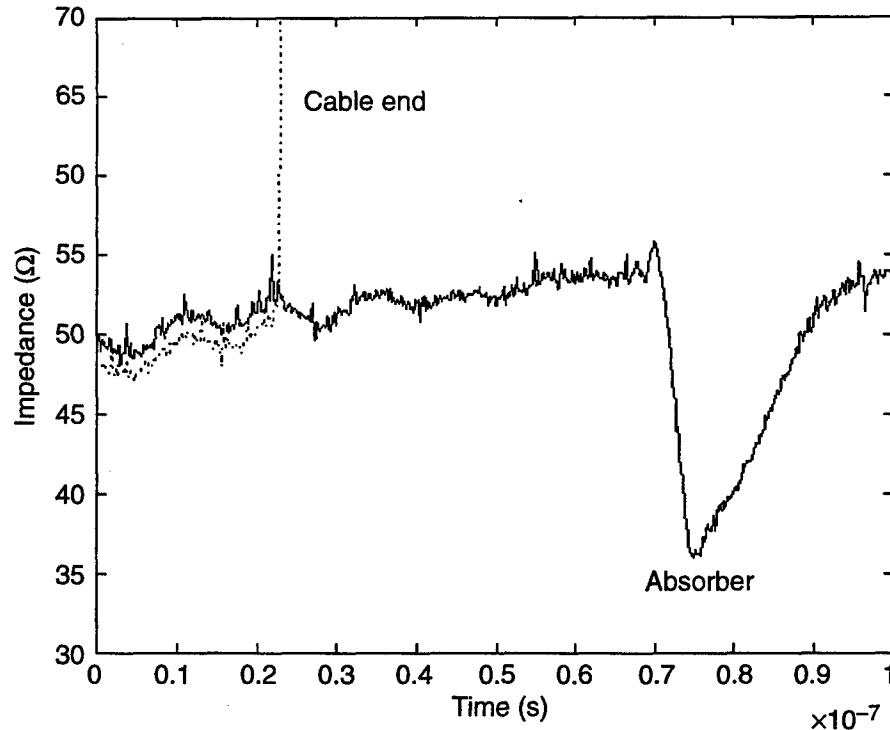


A TDR measurement was performed to determine the impedance characteristics of the G-TEM cell. The results, plotted in figure 4, show a flat impedance until the absorber. The cell begins at the input cable end, which can be seen by the open circuit reflection. Comparison of the curves before the open circuit indicates that the spikes are noise, but the ripple is not. A steady increase in resistance is indicated by the increasing slope. The time window for a measurement would be twice the time from the point of measurement to the absorber reflection. One could determine the point of measurement by shorting the G-TEM cell septum to the shell where the sensor would be placed and noting where the reflection occurs. A less exact rule of thumb is to divide twice the distance to the absorber by the propagation velocity in air of 1 ft/ns. This results in a 20-ns window for this measurement location.

The applied waveform is formed by the output of a coaxial charge line connected by a wetted mercury reed switch to a wave-shaping circuit. The wave-shaping circuit consists of parallel resistors before and after a series capacitor. The resistors bleed off the residual charge between pulses. The pulse is a fast-rise transient with an exponential fall determined by the capacitor. The reed switch coil is operated by commercial 60-Hz ac supplied through a variac.

The pulser output was applied to the G-TEM cell as a source. A Tektronix 7854 digital sampling oscilloscope was used to measure the signal. A Tektronix 7M11 delay line was needed to provide the necessary 75-ns signal delay after triggering. Spurious triggering was occurring on reflected peaks higher than the incident pulse while using the sensor signal as a trigger during a preliminary measurement. We obtained an accurate trigger by splitting the pulser output and using half for a trigger signal and half for the G-TEM source. The exact configuration for applying the signal to the cell was measured through 45 dB attenuation to protect the oscilloscope input. A transfer function was found for the attenuators, oscilloscope cables, and delay line used in the measurement. The pulser output tee and cable to the G-TEM cell were not included in the transfer function, since they are used in the application of the signal to the cell, and any signal deterioration caused by these components should

Figure 4. TDR measurements of G-TEM cell showing 50- Ω cable open and connect to cell.



be included in the corrected data. The applied signals were varied in amplitude to better illustrate the different sensor responses and are plotted in figure 5. The pulses are all close to 4.5 ns wide, which is short enough to avoid reflection problems.

Three sensors were used to measure each electric field transient. The sensors were identical, except for having 10 \times , 5 \times , and no amplification. Each sensor was placed midway between the septum and the floor of the G-TEM cell at the 0.9-m septum height. The sensor cable was routed in the direction of field propagation for a meter and then to the cell wall feedthrough. Care was taken to route the cable perpendicular to the electric field when possible.

The amplifiers were powered through the center conductor by a dc power supply set to supply 60 mA (around 5 V). The dc voltage was blocked from the oscilloscope input by a bias tee. As in the pulser output measurement, the sampling oscilloscope required a 75-ns delay line to properly sample the signal. All the components between the oscilloscope and the sensor were characterized in a transfer function. We made a transfer function for the sensor amplifier using two bias tees and the pins from the sensor with no amplifier, mated to the pins of the sensor with an amplifier. The transfer functions for the amplifiers are shown in figure 6.

The amplifiers, although specified to be flat to 4 GHz, roll off at around 2.5 GHz. The risetime of the applied pulses is averaged to be 135 ps, which is equivalent to an upper band limit of 2.6 GHz. This indicates that some amplifier rolloff may affect the sensor response. A correction for this rolloff was included in the measurement system characteristics correction.

Figure 5.
Measurements of
applied electric fields
corrected for
attenuators, delay line,
cable loss, and 0.9-m
G-TEM cell height.

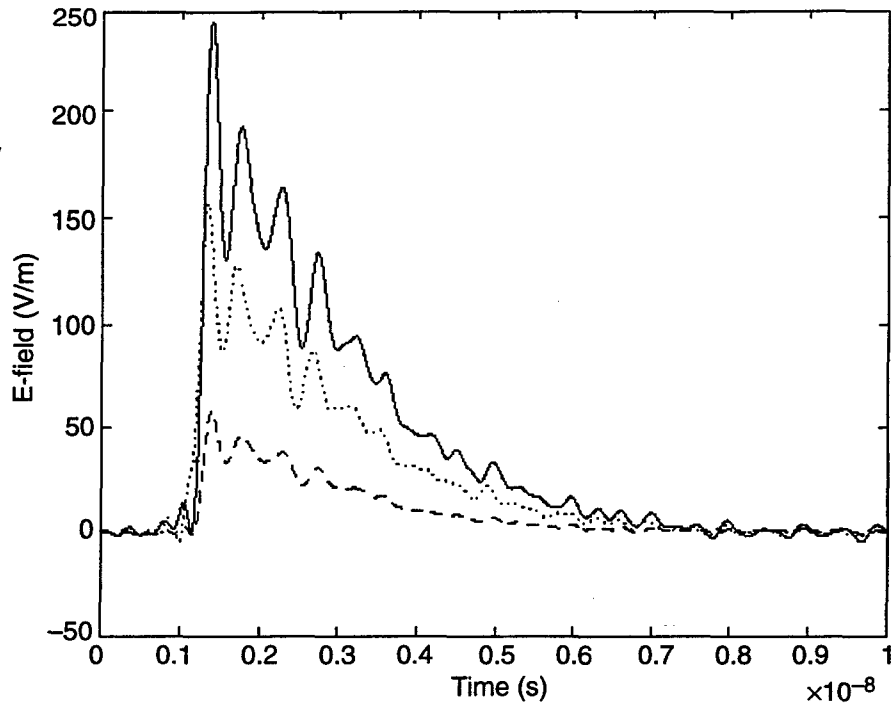
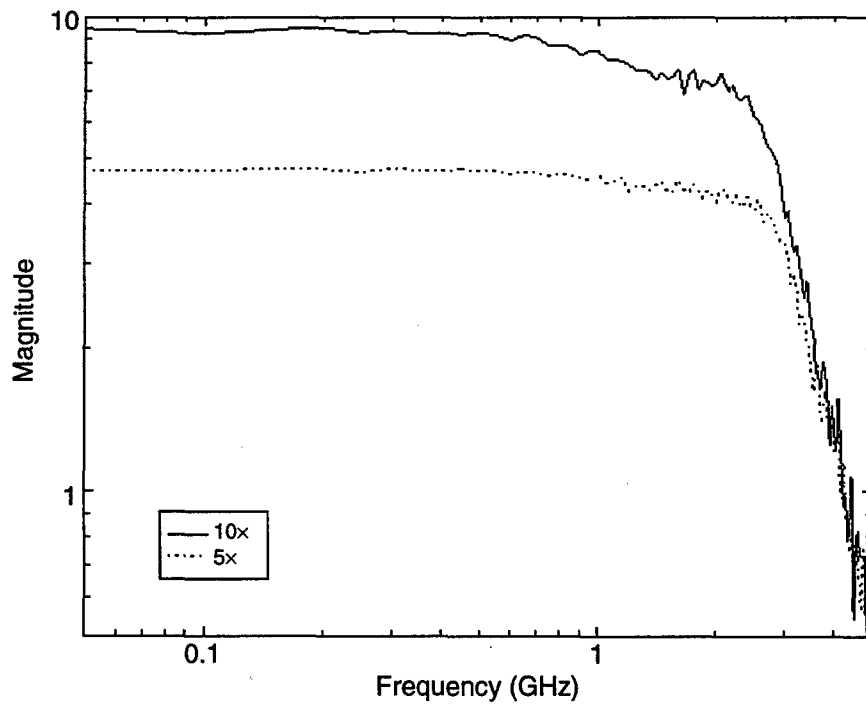


Figure 6. Transfer
function magnitudes
of 10 \times and 5 \times sensor
amplifiers.



There were measurements made with each sensor dipole inverted to allow elimination of common mode noise coupled to the sensor cables. The "down" measurement data (dipole ground leg down) are inverted and added to the "up" data, which eliminate the common mode. The result is divided by two to compensate for the signal data that were added. The data were then corrected for measurement system effects. Care was taken to only invert the dipole sensor without moving the position of the sensor and cable. Care was also taken to not move the sensor and cable location for the three sensor measurements and the three field levels measured.

Next, we calculated the electric field from the corrected data using expressions for electrically small dipoles [4]. An electrically small dipole has an open circuit voltage proportional to the incident electric field parallel to the antenna in the time or frequency domain,

$$V_{oc}(t) = 2h_e E_p^i(t) , \quad (3)$$

where h_e is the equivalent height of the dipole. A relationship for the short-circuit current and a substitution from equation (3) results in

$$I_{sc}(t) = C_a \frac{\partial V_{oc}(t)}{\partial t} = 2h_e C_a \frac{\partial E_p^i(t)}{\partial t} , \quad (4)$$

where C_a is the antenna capacitance. In relation to the very large impedance of an electrically small antenna, the 50- Ω impedance of the measurement system is considered to be a short circuit, which allows the use of equation (4) to relate the measurement to the incident field [4]. A factor of 50 is introduced from $V = I * R$ relation to use the measured voltage data. Equation (4) is integrated on both sides and manipulated to solve for the electric field.

$$E_p^i(t) = \int \frac{\partial E_p^i(t)}{\partial t} dt = \frac{\int V(t) dt}{A_{eq} \epsilon_0 Z_c} , \quad (5)$$

where A_{eq} is called the equivalent area and is related to the physical characteristics that define the dipole and antenna capacitance. The cable impedance Z_c is 50 Ω and E_p^i is the electric field parallel to the dipole. The variables defining the physical characteristics are calculated [5]

$$\begin{aligned} A_{eq} &= \frac{C_a h_e}{\epsilon_0} \\ h_e &= \frac{h(\Omega - 1)}{\Omega - 2 + \ln(4)} \\ C_a &= \frac{2\pi h \epsilon_0}{\Omega - 2 - \ln(4)} \\ \Omega &= 2 \ln\left(\frac{2h}{a}\right) , \end{aligned} \quad (6)$$

where h is the half dipole length and a is the dipole radius. The results of the calculations for the electric field of the 10× and the 5× sensors were multiplied by constants of 1.3 and 1.1, respectively. This was to match them to the G-TEM field being used to calibrate the sensors. This small adjustment is compensation for differences between ideal dipole models and the real world. The MATLAB routine written to perform this series of calculations is shown in appendix C.

5. Results

The measured voltage data from the dipoles placed in the G-TEM electric field were corrected, integrated, and used in equation (5) to calculate the measured electric field. The measured electric field was compared with the G-TEM field at the measurement location. The results are shown in figures 7, 8, and 9.

Figure 7. Fields calculated from measured dipole voltage compared with 245-V G-TEM field at measurement location. Comparison is in (a) time and (b) frequency domains. Constant factors of 1.3 and 1.1 are used to compensate for inaccuracies in dipole model predictions for 10× and 5× sensors, respectively.

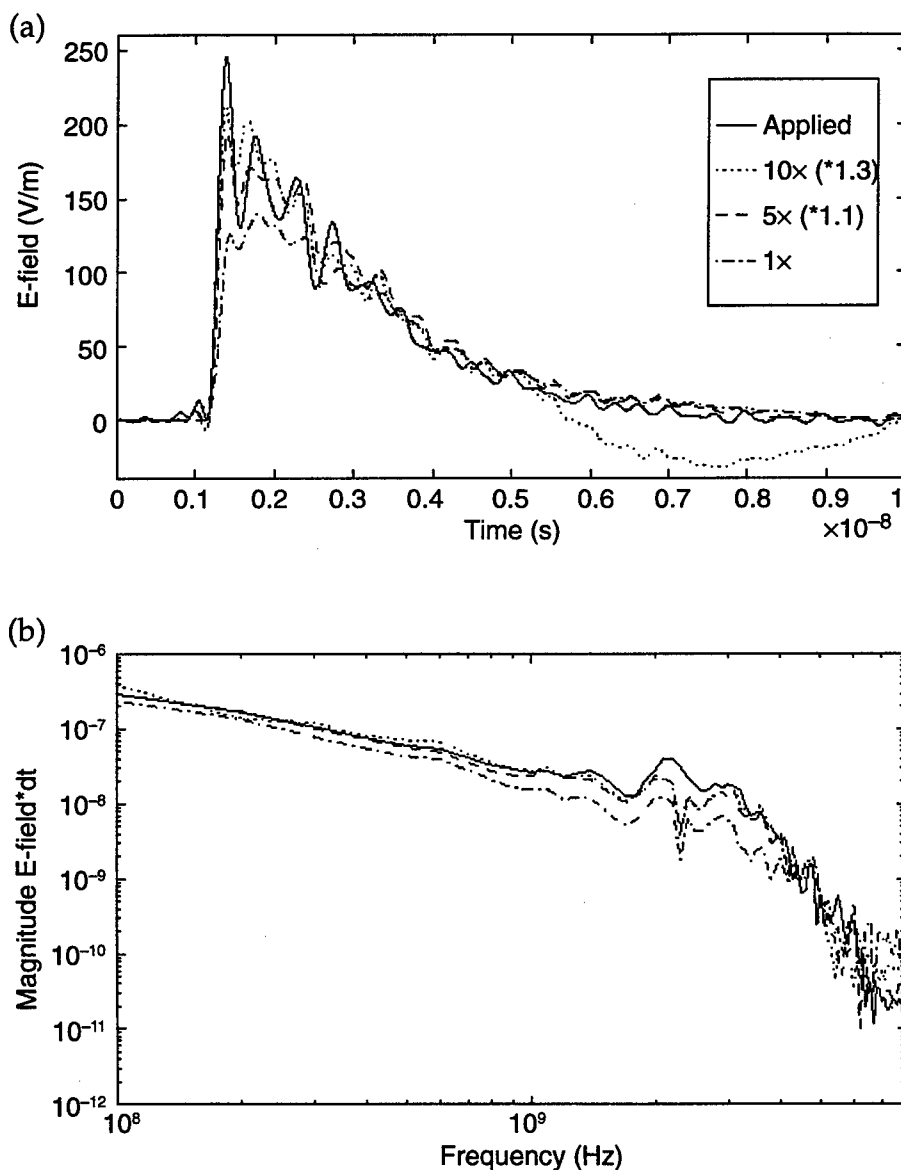


Figure 8. Fields calculated from measured dipole voltage compared with 155-V G-TEM field at measurement location. Comparison is in (a) time and (b) frequency domains. Constant factors of 1.3 and 1.1 are used to compensate for inaccuracies in dipole model predictions for 10× and 5× sensors, respectively.

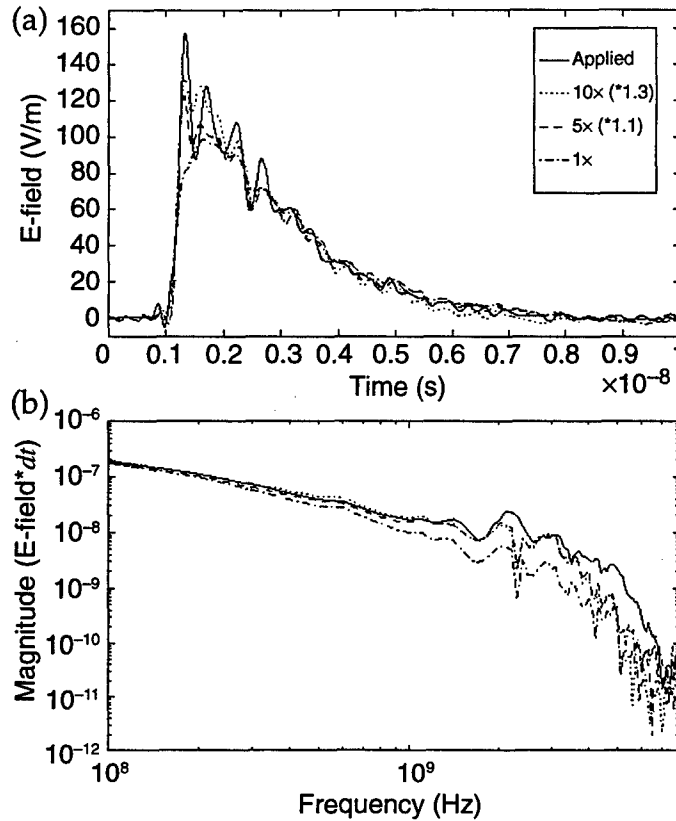
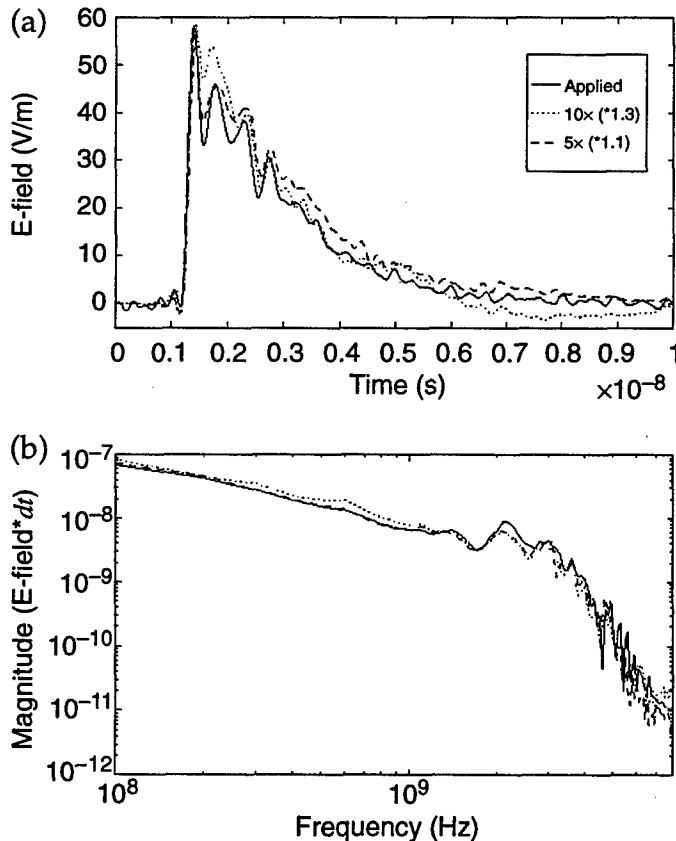


Figure 9. Fields calculated from measured dipole voltage compared with 60-V G-TEM field at measurement location. Comparison is in (a) time and (b) frequency domains. Constant factors of 1.3 and 1.1 are used to compensate for inaccuracies in dipole model predictions for 10× and 5× sensors, respectively.



The comparison shows an improvement in the high-frequency characteristics with increased amplification. A smaller improvement was seen between the 10× and 5× sensors because they both increased the portion of the signal lost to cable attenuation above the noise floor. A much smaller signal would be needed to begin degrading the amplified sensor response noticeably. The rolloff of the amplifiers at 2.5 GHz causes some loss of the initial E-dot data, because the upper limit of the differential field frequency content is twice that of the electric field. This is obvious because, by definition, the differential field has its peak around the middle of the risetime of the electric field. As mentioned earlier, the applied pulses have frequency content up to 2.6 GHz. Using the reasoning above, the E-dot signal would have an upper frequency content of around 5 GHz. The frequency content between 2.5 and 5 GHz was not amplified consistently, and the transfer function for the amplifier had to be applied to correct inconsistencies. The cable losses present at the frequencies not amplified decreased some of the signal below the measurement sensitivity of the equipment. This lost information would cause the applied transfer function to lose accuracy. This would account for the inability to measure the same peak value as the G-TEM field and the loss of some of the structure in the transient. Even with the amplifier's capabilities being exceeded, the data show an increase in accuracy over the nonamplified dipole.

Figure 10 is an E-dot data plot of the 60 V/m peak field measured with the 5× dipole. The upper plot of figure 10 also shows the common mode noise caused by fields coupling to the sensor cable. The common mode signal is present at the dipole, where it combines with the ground leg portion of the dipole signal. Inverting the dipole inverts the dipole response, while the common mode noise remains the same. This allows us to remove the noise by inverting the inverted signal digitally, adding, and dividing by two to correct the amplitude. The result of this process is shown in the lower plot.

Figure 11 compares the E-dot data from the 10×, 5×, and 1× sensors. With the extrapolation of the nonamplified sensor response peaks from field transients with peaks of 245 and 155 V/m in the bottom plot of figure 11, the measurement of the field transient with a peak of 60 V/m should provide a sensor response peak of around 8 mV. A measurement of the 60 V/m peak field transient with the unamplified dipole was not possible with the available scope sensitivity.

Assuming a minimum usable transient peak amplitude of 10 mV, we can use the E-dot sensor response peaks in the top and middle plots of figure 11 to determine the field level that would result in a 10-mV peak. If we assume linearity, the ratio of a measured E-dot sensor peak response to the G-TEM field times the minimum measurable peak response of 10 mV should provide the minimum field measurable by that sensor. The application of this proportionality to the 5× sensor data results in a minimum measurable field peak of 13 V/m from an average of the three measurements with the sensor. The 10× sensor minimum measurable field peak is 8 V/m.

Figure 10. Sensor response: (a) Raw dipole response for ground leg down and up. Measurement was made with 5 \times sensor placed in 60 V/m peak electric field. (b) Result of combining two data sets to remove noise.

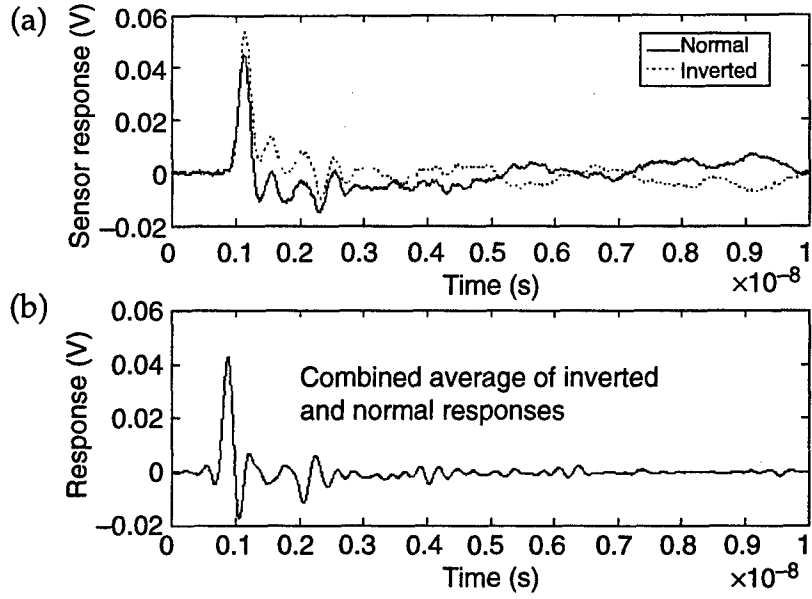
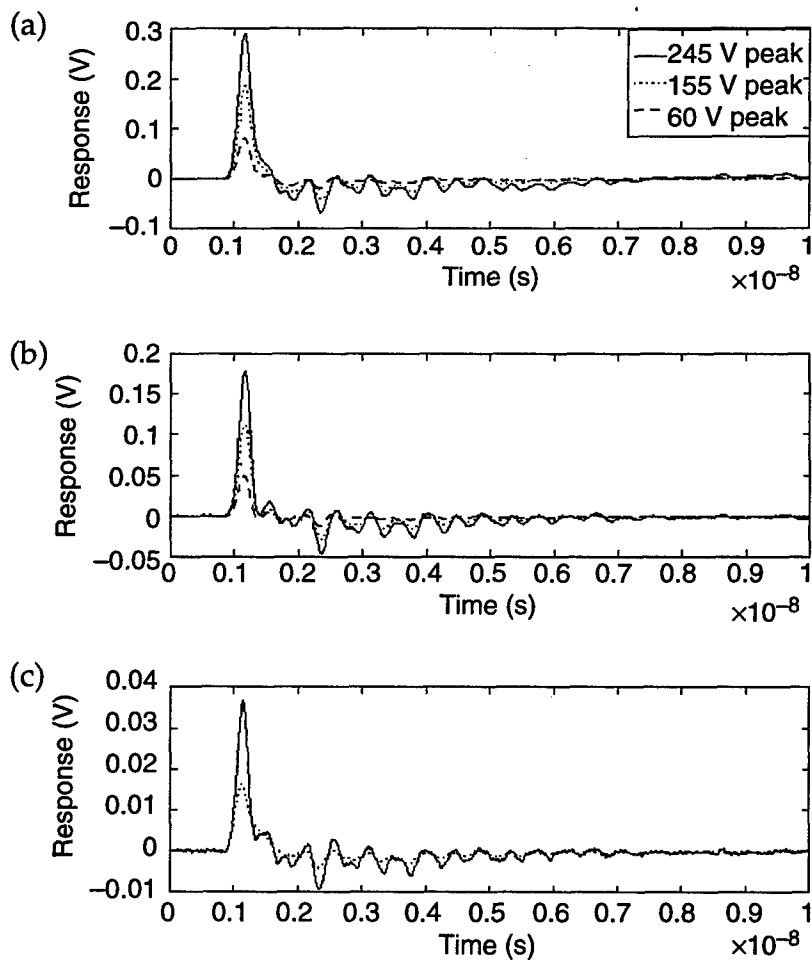


Figure 11. Results of E-dot data with common mode noise removed in G-TEM fields with (a) 10 \times , (b) 5 \times , and (c) no amplifier. An individual sensor's response to different G-TEM fields is compared in each plot.



The peak amplitudes of the 10× and 5× sensors would differ by a factor of two if the amplification was flat in the frequency domain. We find a factor of around 1.7 by inspecting for the difference in peak amplitudes from the 10× and 5× sensors. This agrees with the value of 1.75 we find by averaging the result of dividing the transfer function for the 10× amplifier by the transfer function for the 5× amplifier and restricting the data to below 3 GHz. The 10× sensor data have a peak amplitude factor of around 8 with respect to the nonamplified sensor response.

As the measured amplitudes near the lower bound of sensitivity, there is loss of structure in the time-domain signal and a corresponding loss of frequency content. The structure loss occurs when the lower amplitude peaks are lost in the noise of a time-domain measurement. If the amplification at the sensor is constant in the frequency domain, the minimum measurable unamplified signal is increased by the amplification factor. The amplified signal will still suffer degradation as it nears the improved lower bound of sensitivity.

A resonance in the frequency domain can be seen in the frequency response plots of the sensors (fig. 6–8) at around 2.1 GHz. This is a result of the construction of the sensors and can be minimized with modifications. The suspect area would be the dipole gap where stray capacitances or inductances could occur. The fact that the resonance is not as dramatic for the measurements in the lowest field levels could indicate a higher noise floor.

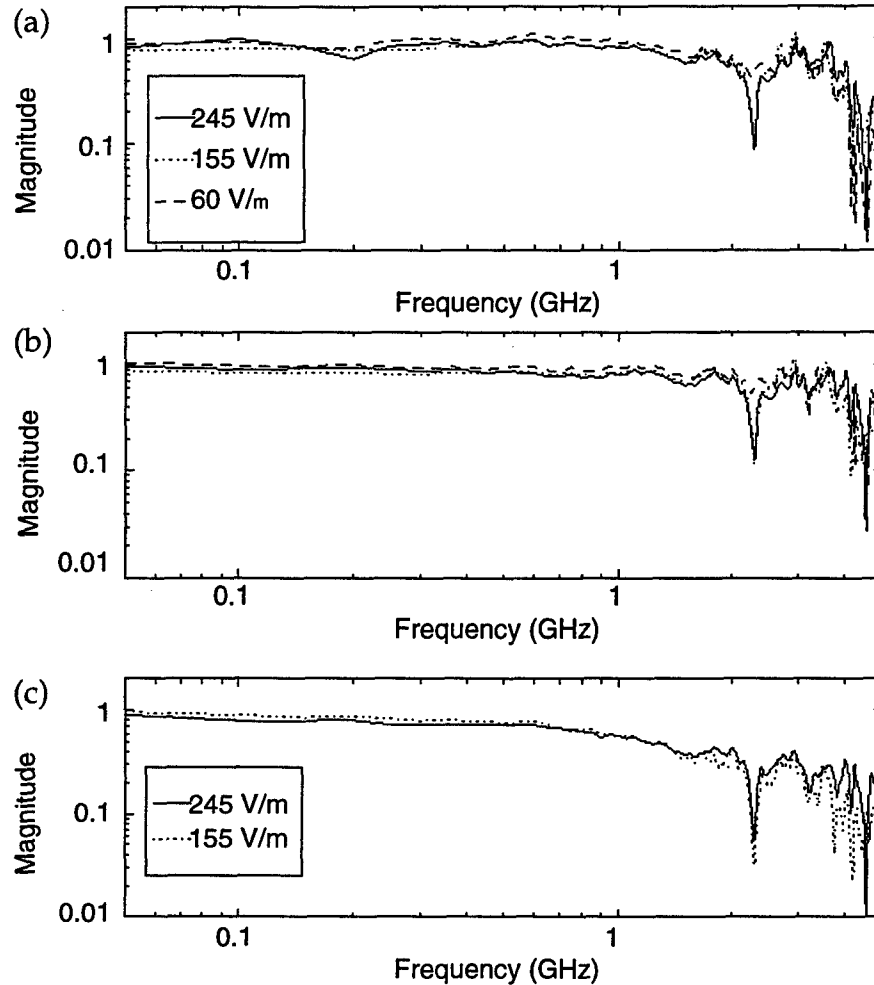
Fabrication methods could be improved for the amplifier installation. Heat limits were probably exceeded when the coax shield was soldered. This could explain the loss of amplification above 2.6 GHz when the specifications are 4 GHz. Same-size amplifiers with upper limits at 6 GHz are manufactured by the same manufacturer. A stable 65-mA current controlled voltage source could be made to reduce small errors due to inconsistent voltage supply.

The sensor response in the frequency domain with the measurement system and amplification removed is shown in figure 12. The rolloff at the high-frequency end is the result of filtering to remove large oscillations caused by noise.

6. Conclusions

The amplifier incorporated into the sensor improves the measurement system sensitivity and accuracy by the performance of the amplifier. We avoid any signal degradation due to measurement system characteristics by amplifying the signal before it can be affected. An improvement in the fabrication methods and choice of amplifier that produces flat response in the frequency domain being measured can improve the accuracy of the sensor. The sensors used in the experiment show improvement in sensitivity and accuracy over the nonamplified sensor, despite inconsistent

Figure 12. Transfer functions for three sensors used in experiment, corrected for frequency characteristics of measurement system and amplifiers in sensor with (a) 10 \times , (b) 5 \times , and (c) no amplifier. Each plot contains result of indicated sensor's response to G-TEM field convolved with the G-TEM field in frequency domain.



amplification in the measurement frequency band. An increase in sensitivity was shown, from above 60 to 13 V/m for the 5 \times sensor and 8 V/m for the 10 \times sensor.

The feature of pin connectors in the sensor allows for flexibility in its use. For example, an H-field sensor could be made using a small loop in place of the dipole. For cw measurements, we could enhance the sensitivity of the sensor by sizing the antenna to be resonant. This would vastly improve the antenna response above that of the electrically small antenna necessary for time domain measurements.

The size of the sensor is minimized to the dipole and the semirigid coaxial measurement cable. This minimum size reduces the perturbation of the field being measured by the presence of the sensor. The symmetry of the sensor allows scattered fields incident from above and below the sensor to be measured without interference. Ground plane sensors cannot accurately perform these measurements. The symmetry also permits the sensor to be inverted to provide the data that allow removal of common-mode noise from the sensor response.

More complicated circuits could be made small enough to remain in the electrically small category and provide a high impedance for direct electric field measurements, antenna loading, etc. The miniaturization of electronic components makes what was improbable a few years ago a possibility today.

References

1. Shaarawi, Amr M., and Sedki M. Riad, "Spectrum Amplitude of Step-Like Waveforms Using the Complete-FFT Technique," *IEEE Trans. Instrum. Meas.* **IM-34**, 4, December 1985.
2. Riad, Sedki M., and Robert B. Stafford, "Impulse Response Using Frequency Domain Optimal Compensation Deconvolution," *Proc. 23rd Midwest Symp. on Circuits and Systems*, Toledo, OH, 521-525, August 1980.
3. The Electro-Mechanics Company, *G-TEM! Model 5300 Series Operation Manual*, 1993.
4. Messier, Michael A., *Coupling to Antennas*, DNA 2114 EMP handbook revision, chapter 10.
5. Kanda, Motohisa, "Standard Probes for Electromagnetic Field Measurements," *IEEE Trans. Antennas Propag.* **41**, 10, October 1993.

Appendix A.—MATLAB Function CALSTEP

This appendix gives the MATLAB routine M-file calstep.m, which is the source for the function calstep. The function calstep uses measured time-domain data for component input and output to create a component transfer function by employing an optimal deconvolution method in an iterative fashion. Progress toward a solution is determined using a graphic interface and knowledge of the frequency content of the applied waveform.

```
% b = the input signal
% a = the output signal
% c = the transfer function
%
% function ccc = calstep(b,a)
%
% check the inputs to see if they are a power of two and
% equally spaced. If not, interpolate to a power of two
% which also matches the waveforms point for point.
%
function ccc = calstep(b,a)

% First, ensure the first point is zero time and amplitude
if a(1,1) ~= 0, a(1,1) = 0.0; end
if a(1,2) ~= 0, a(1,2) = 0.0; end
if b(1,1) ~= 0, b(1,1) = 0.0; end
if b(1,2) ~= 0, b(1,2) = 0.0; end
nb = length(b);
na = length(a);
tb = b(nb,1);
ta = a(na,1);
intpl=0;
xx=diff(b(:,1));
    if (1 - min(xx) / max(xx)) > .01
        disp(' Need equally spaced points in the input data')
        disp(' The points will be interpolated to the smallest dt')
        intpl=1;
    end
dtmin = min(xx);
xx=diff(a(:,1));
    if (1 - min(xx) / max(xx)) > .01
        disp(' Need equally spaced points in the output data')
        disp(' The points will be interpolated to the smallest dt')
        intpl=1;
    end
end
dta = min(xx);
if dta < dtmin
    dtmin = dta;
```

Appendix A

```
end
nmax=nb;
while log2(nmax) > fix(log2(nmax))
    disp('Need a power of two data points, will interpolate')
    disp(['Total points now are ',num2str(nmax)])
    nmax=input('How many points do you want?')
    dtmin = tb/(nmax-1);
    intpl=1;
end
tmax=tb;
t = dtmin * (0:nmax-1)';
if tb > ta
    disp(' Need equal length data sets, input is longer')
    disp(' The data will be interpolated to the shortest length')
    nmax = fix(ta/dtmin) + 1;
    if log2(nmax) > fix(log2(nmax))
        disp('Need a power of two data points, will interpolate')
        nmax =pow2(fix(log2(nmax))+1);
        dtmin = ta/(nmax-1);
    end
    tmax = (nmax-1) * dtmin;
    t = dtmin * (0:nmax-1)';
    intpl=1;
end
if ta > tb
    disp(' Need equal length data sets, output is longer')
    disp(' The data will be interpolated to the shortest length')
    nmax = fix(tb/dtmin)+1;
    if log2(nmax) > fix(log2(nmax))
        disp('Need a power of two data points, will interpolate')
        nmax =pow2(fix(log2(nmax))+1);
        dtmin = tb/(nmax-1);
    end
    tmax = (nmax-1) * dtmin;
    t = dtmin * (0:nmax-1)';
    intpl=1;
end
if intpl == 1
    sa = interp1(a(:,1),a(:,2),t);
    sb = interp1(b(:,1),b(:,2),t);
else
    sa = a(:,2);
    sb = b(:,2);
end
subplot(2,1,1)
plot(a(:,1),a(:,2),t,sa)
title('Output')
subplot(2,1,2)
plot(b(:,1),b(:,2),t,sb)
```

```

title('Input')
figure(1)
pause(2)
%
% The Nicolson ramp method and the Gans-Nahman inverse waveform
% method are used here.
% The Nicolson ramp method uses a ramp "ra" created using the number
% of points "na" and the amplitude of the final point:
n = 0:1:nmax-1;
ra = (n/(nmax-1) * sa(nmax))';
rb = (n/(nmax-1) * sb(nmax))';
sra = sa - ra;
srb = sb - rb;
subplot(2,1,1)
plot(t,sra)
title('Output ramped to 0')
subplot(2,1,2)
plot(t,srb)
title('Input ramped to 0')
figure(1)
pause(2)
sram = fft(sra);
srbm = fft(srb);
f = (0:1/t(nmax):1/((t(2)-t(1))*2))';
subplot(2,1,1)
sam=abs(fft(sa));
loglog(f,abs(sram(1:length(f))),f,sam(1:length(f)))
title('ramp FFT vs FFT for output')
subplot(2,1,2)
sbm=abs(fft(sb));
loglog(f,abs(srbm(1:length(f))),f,sbm(1:length(f)))
title('ramp FFT vs FFT for input')
figure(1)
pause(2)
%
% The Gans-Nahman inverse waveform method appends an inverse
% waveform "u" to the last point of the original waveform.
%
ua = sa(nmax) - sa;
ub = sb(nmax) - sb;
sua = [sa ; ua];
sub = [sb ; ub];
tu = 0:(2 * tmax/(2 * nmax - 1)):2 * tmax;
subplot(2,1,1)
plot(tu,sua)
title('Output for Gans-Nahman invers waveform FFT')
subplot(2,1,2)
plot(tu,sub)
title('Input for Gans-Nahman invers waveform FFT')

```

Appendix A

```
figure(1)
pause(2)
suam = fft(sua) * 0.5;
subm = fft(sub) * 0.5;
f = (0:1/tu(2 * nmax):1/((tu(2)-tu(1))*2))';
%
% Replace the even function series of the Gans-Nahman method
% with the values calculated in the Nicolson method. This
% would replace the erroneous even values caused by the
% frequency spacing. The DC value is correct for the Gans-Nahman
% method and will remain.
%
K=3;
cma=suam;
for k = 1:nmax-1
    cma(K) = sram(k+1);
    K=K+2;
end
K=3;
cmb=subm;
for k = 1:nmax-1
    cmb(K) = srbm(k+1);
    K=K+2;
end
subplot(2,1,1)
loglog(f,abs(cma(1:nmax)))
title('Combined Gans-Nahman inverse and ramp method FFT for Output')
subplot(2,1,2)
loglog(f,abs(cmb(1:nmax)))
title('Combined Gans-Nahman inverse and ramp method FFT for Input')
figure(1)
pause(2)
%
% Perform the division of output over input to obtain the transfer
% function for the common period and the smallest dt of the input
% and output functions.
%
% This is done using a deconvolution algorithm.
%
% or by simply dividing
%
c = cma ./ cmb;
c(1) = 0;
% assumes a DC content of zero in the transfer function
%
subplot(1,1,1);

rta=risetime(a);
pause(2)
```

```

rtb=risetime(b);
pause(2)
rtfa=.35/rta;
rtfb=.35/rtb;
close(1)
nrtfa=max(find(f < rtfa))+1;
nrtfb=max(find(f < rtfb))+1;
crta=[min(abs(c(2:nrtfa)))/10 10*max(abs(c(2:nrtfa)))];
crtb=[min(abs(c(2:nrtfb)))/10 10*max(abs(c(2:nrtfb)))];

% using the deconvolution algorithm
% With an iteration program to specify G
f = (0:1/tu(2 * nmax):1/((tu(2)-tu(1))))';

maxfreq=1/(dtmin*10);
fnum=min(find(f >= maxfreq));
G = input('Enter a value for the iteration ');
%
figure(1)
subplot(1,1,1);
while G ~= 0
    CFILTER=conj(cmb) ./ (abs(cmb) .^ 2 + G);
    CF = cma .* CFILTER;
    CF(1) = 0;
% assumes a DC content of zero in the transfer function

loglog(f(1:nmax),abs(CF(1:nmax)),f(1:nmax),abs(c(1:nmax)),...
[rtfa rtfa],crta,'-',[rtfb rtfb],crtb,':')
    axis([f(1) f(nmax) crta]);
    pause(1)
    title(['Enter value or 0 to quit, Base Risetime freq =
',num2str(rtfb)])

    GG=G;
    figure(1)
    G = input('Enter a value for the iteration, 0 to quit ');
end

%
%
loglog(f(1:nmax),abs(CF(1:nmax)),f(1:nmax),abs(c(1:nmax)))
title(['Convolution with constant ',num2str(G),' vs constant = 0'])
pause(2)

loglog(f(1:fnum),abs(CF(1:fnum)), [rtfa rtfa],crta,'-', [rtfb
rtfb],crtb,':')
title('Cal curve plotted to the frequencies with >10 points in the
risetime')
ccc=[f CF];

```

Appendix B.—MATLAB Function CAL

This appendix gives the MATLAB routine M-file cal.m, which is the source for the function cal. The function cal allows measured data to be "calibrated" or to have the effects of the frequency-domain characteristics of the measurement system components contained in a transfer function to be removed. The transfer function is created with calstep.m, the MATLAB function given in appendix A of this report.

```
% This function takes a transfer function "tfn" that has been ob-
% tained using
% the function calstep on two equal length time files that describe
% the
% response of the system with and without the portion being cali-
% brated and
% applies it to the measured signal "s". "s" must be the same length
% as the
% transfer function time files
%
%
% function sysresp = cal(tfn,s)
%
%
% check the inputs to see if they are a power of two and equally
% spaced. If not, interpolate to a power of two which also
% matches the waveforms point for point.
%
function sysresp = cal(tfn,s)
%
% First, ensure the first point is zero time and amplitude
if s(1,1) ~= 0, s(1,1) = 0.0; end
if s(1,2) ~= 0, s(1,2) = 0.0; end
sa=s(:,2);
t=s(:,1);
ns = length(sa);
%
%
xx=diff(s(:,1));
if (1 - min(xx) / max(xx)) > .01
    disp(' Need equally spaced points in the input data')
    disp(' The points will be interpolated to the smallest dt')
    intpl=1;
    pause(2)
end
dtmin = mean(xx);
if log2(ns) > fix(log2(ns))
    disp('Need a power of two data points, will interpolate')
    ns =pow2(fix(log2(ns))-1);
```

Appendix B

```
    dtmin = s(length(s),1)/(ns-1);
    t = dtmin * (0:ns-1)';
    sa = interp1(s(:,1),s(:,2),t);
end
%
% The Nicolson ramp method and the Gans-Nahman inverse waveform
% method are used here.
% The Nicolson ramp method uses a ramp "ra" created using the number
% of points "n" and the amplitude of the final point:
%
n = 0:1:ns-1;
ra = (n/(ns-1) * sa(ns))';
sra = sa - ra;
plot(s(:,1),s(:,2),t,sra,'.')
title('Original data versus data ramped to zero')
figure(1)
pause(2)
sram = fft(sra);
f = (0:1/t(ns):1/((t(2)-t(1))*2))';
sam=abs(fft(sa));
loglog(f,abs(sram(1:length(f))),f,sam(1:length(f)))
title('Nicolson ramp FFT vs regular FFT')
figure(1)
pause(2)
%
% The Gans-Nahman inverse waveform method appends an inverse
% waveform "u" to the last point of the original waveform.
%
ua = sa(ns) - sa;
sua = [sa ; ua];
tu = dtmin * (0:2*ns-1);
plot(tu,sua)
title('The Gans-Nahman inverse waveform to be FFTed')
figure(1)
pause(2)
suam = fft(sua) * 0.5;
f = (0:1/tu(2 * ns):1/((tu(2)-tu(1))*2))';
%
%
% Replace the even function series of the Gans-Nahman method with
the
% values calculated in the Nicolson method. This would replace the
% erroneous even values caused by the frequency spacing. The DC
value
% is correct for the Gans-Nahman method and will remain.
%
K=3;
sf=suam;
for k = 1:ns-1
```

```

        sf(K) = sram(k+1);
        K=K+2;
    end
    subplot(1,1,1)
    loglog(f,abs(sf(1:length(f))),tfn(:,1),abs(tfn(:,2)))
    title('Resulting combination of signal FFTs vs transfer function')
    figure(1)
    pause(2)
%
%
%
    tf=tfn(:,2);
%
%   Perform the division of output over input to obtain the transfer
%   function for the common period and the smallest dt of the input
%   and output functions.
%
%   This is done using a deconvolution algorithm.
%
%   or by simply dividing
%
    c = sf ./ tf;
    rt=risetime(s);
    pause(2)
    rtf=.35/rt;
    close(1)
    nrtf=max(find(f < rtf))+1;
    crt=[min(abs(c(2:nrtf)))/10 10*max(abs(c(2:nrtf)))];
%
%   using the deconvolution algorithm
%   With an iteration program to specify G

    maxfreq=1/(dtmin*10);
    fnum=min(find(f >= maxfreq));

    G = input('Enter a value for the iteration');
%
    subplot(1,1,1);
    while G ~= 0
        CFILTER=conj(tf) ./ (abs(tf) .^ 2 + G);
        CF = sf .* CFILTER;
        loglog(f(1:ns),abs(CF(1:ns)),f(2:ns),abs(c(2:ns)), [rtf
rtf],crt,':')
        axis([f(1) f(ns) crt]);
        pause(1)
        title(['Enter value or 0 to quit, Risetime freq =
',num2str(rtf)])
        GG=G;
        figure(1)
    end

```

Appendix B

```
G = input('Enter another value for the iteration, 0 to quit ');
end

loglog(f(1:fnum),abs(CF(1:fnum)),[rtf rtf],crt,':')
sysres = ifft(CF);
title('Risetime Frequency is dotted line')
sysresp=[t real(sysres(1:length(t)))+ra];
figure(1)
pause
disp(['The maximum imaginary part of the IFFT is:',
num2str(max(imag(sysres)))])
plot(sysresp(:,1),sysresp(:,2))
figure(1)
pause(2)
```

Appendix C.—Data Correction Algorithm

This is the algorithm used to correct the data for measurement system characteristics, remove common-mode noise, and calculate the field from the dipole dimensions. The other routines called in this file are included at the end of this appendix.

```
% This routine accelerates the process of using the dipole
% inverted and not inverted signal to remove common mode cable
% signals. The measurement must be calibrated to remove
% measurement system characteristics. The antenna amplifier at
% the dipole can be treated as a constant or the characteristics
% can be included in with the measurement system. The signal with
% the ground leg up is shifted to remove DC offset, inverted,
% shifted to match risetimes, added together and divided by 2,
% corrected, integrated, then the E-field proportional to the
% measured voltage is calculated from dipole dimensions for an
% electrically small antenna.
%
% input needed is:
%
% sup      = measured input signal with dipole shield leg up
% sdn      = measured input signal with dipole shield leg down
% tcbl     = transfer function of measurement system previously
determined
% rdipole = dipole radius in meters
% hdipole = dipole half height in meters
%
% function aaa=cdipole(sup, sdn, tcbl, rdipole, hdipole);
%
%
function aaa=cdipole(1, sdn, tcbl, rdipole, hdipole, amp);
% Remove cable losses using transfer functions generated with
calstep
% First remove any DCoffset
sup=dcoffset(sup);

sdn=dcoffset(sdn);

% invert the reversed measurement

aaa=sup;
aaa(:,2)=-sup(:,2);

disp('Now you must line up the rise times of the signals')
pause(2)

aaa=shifty(aaa, sdn);
```

Appendix C

```
% add the data and divide by two, this removes common mode
noise bbb=aaa;
bbb(:,2)=(aaa(:,2)+sdc(:,2))/2;

% set first and last point to zero

bbb(1,2)=0;
bbb(1,2)=0;

ccc=cal(tcbl, bbb);

ddd=shiftint(ccc);
pause(2)

% now the antenna Aeq is calculated
close(1)
pause(1)

eps0=8.854e-12;
omega=2*log(2*hdipole/rdipole);
disp(['Antenna fatness factor is ', num2str(omega)])

heq=hdipole*(omega-1)/(omega-2+log(4));
disp(['Antenna equivalent height is ', num2str(heq)])

Ca=2*pi*hdipole*eps0/(omega-2-log(4));
disp(['Antenna capacitance is ', num2str(Ca)])

Aeq=Ca/eps0*heq;
disp(['Antenna equivalent area is ', num2str(Aeq)])

pause(3)

% calculate incident field
eee=ddd;
eee(:,2)=ddd(:,2)/(eps0*Aeq*50);

plot(eee(:,1),eee(:,2))
title(['Measured E-field with dipole '])
xlabel('Seconds')
ylabel('Volts/Meter')

%*** DCOFFSET.M ***

%
% This function shifts the Y values up or down by the mean of
% the baseline data, The amount of baseline used is determined
% visually.
```

```

% The data must be two columns of X, Y values
%
% b = the curve to be shifted
% a = the baseline to be averaged
%
function sh = dcoffset(b)
a=b;
plot(b(:,1),b(:,2),a(:,1),a(:,2))
title('Input the begining and end points in the baseline to be used
')
grid
figure(1)
disp('***** Enter end = 1 to quit *****')
ns = input('Input the begining point in the baseline to be used ');
ne = input('Input the end point in the baseline to be used ');

while ne > 1
    if ns == 0, ns = 1; end
    if ne == 0, ne = 1; end
    a = b(ns:ne,:);
    plot(b(:,1),b(:,2),a(:,1),a(:,2))
    title('Input the begining and end points in the baseline to be
used')
    grid
    figure(1)
    nns=ns;
    ns = input('Input the begining point in the baseline to be used
');
    ne = input('Input the end point in the baseline to be used ');
end
ave=mean(a(:,2));
sh=b;
sh(:,2)=b(:,2)-ave;
sh(1:nns,2)=sh(1:nns,2)*0;
plot(sh(:,1),sh(:,2))
title('Shifted to eliminate DC offset')
figure(1)

%*** SHIFTINT.M ***

% this routine combines shiftx.m and funint.m into a loop to allow
the
% interactive removal of DC bias
%
%
% This function shifts the Y values up or down while plotting the
% reference and shifted curves for comparison
% The data must be two columns of X, Y values
%

```

Appendix C

```
% b = the curve to be shifted
%
function c = shiftint(b)
a=b;
c=funint(b);
plot(c(:,1),c(:,2))
title('The integrated unshifted curve')
figure(1)
pause
title('***Enter value to shift curve +up or -down***')
pause(2)
plot(b(:,1),b(:,2),a(:,1),a(:,2))
title('Enter value to shift curve +up or -down');
figure(1)
grid
ns = input('Input the value to shift y values up or down ');
sh = b;
while ns ~= 0
    sh(:,2) = ns + b(:,2);
    c=funint(sh);
    plot(c(:,1),c(:,2))
    title('The integrated shifted curve, Enter value to shift again')
    figure(1)
    ns = input('Input the value to shift y values up or down ');
end
c=funint(sh);
plot(c(:,1),c(:,2))
title('The final integrated shifted curve')
figure(1)
```

```
*** SHIFTY.M ***
```

```
%
% This function shifts the Y values to the right while plotting the
% reference and shifted curves for comparison
% The data must be two columns of X, Y values
%
% b = the curve to be shifted
% a = the reference curve
%
function sh = shifty(b, a)
plot(b(:,1),b(:,2),a(:,1),a(:,2))
title('Enter # of spaces to shift yellow curve +right or -left');
figure(1)
nstag = input('Enter # of spaces to shift yellow curve +right or -left');
np = length(b);
while nstag ~= 0
    ns=nstag;
```

```

sh(:,1) = b(:,1)+(b(2,1)*(ns-1));
sh(:,2) = b(:,2);
plot(sh(:,1),sh(:,2),a(:,1),a(:,2))
title('# of spaces to shift yellow curve +right or -left');
figure(1)
nstog = input('Enter # of spaces to shift yellow curve +right or -
left');
end
sh(:,1)=b(:,1);
sh(:,2) = b(:,2)*0;
if ns > 0
    sh(ns+1:np,2) = b(1:(np-ns),2);
else
    ns=abs(ns);
    sh(1:(np-ns),2) = b(ns+1:np,2);
    sh(np-ns+1:np,2) = sh(np-ns+1:np,2)*0+sh(np-ns,2);
end
plot(sh(:,1),sh(:,2),a(:,1),a(:,2))
title('Final shifted curve')
figure(1)

```

```

%*** RISETIME.M ***

```

```

% This routine finds the peak and computes the 10 to 90 percent
risetime
%
% Input the signal variable - s
% function a=risetime(s)

function dxr=risetime(s)
%
plot(s(:,1),s(:,2))
title('Place cursor at begining of risetime peak, click left button')
aaa=ginput(1);
xs=aaa(1);
title('Place cursor at end of risetime peak, click left button')
aaa=ginput(1);
xe=aaa(1);
ns=max(find(s(:,1) <= xs));
ne=max(find(s(:,1) <= xe));
plot(s(:,1),s(:,2),s(ns:ne,1),s(ns:ne,2))
title('Selected area in which to find risetime')
pause(2)

%
% Determine peak absolute value
np = ne-ns+1;
peak = 0.0;
for I=ns:ne

```

Appendix C

```
    if abs(s(I,2)) > abs(peak)
        peak=s(I,2);
        npk=I;
        tp=s(I,1);
    end
end
%
%   COMPUTE RISETIME OF PEAK
%
ys = abs(peak) * 0.1;
ye = abs(peak) * 0.9;
nye=max(find(abs(s(ns:ne,2)) <= ye & s(ns:ne,1) < tp))+(ns-1);
nys=max(find(abs(s(ns:ne,2)) <= ys & s(ns:ne,1) < tp))+(ns-1);
dy=abs(s(nye,2)-s(nys,2));
dx=s(nye,1)-s(nys,1);
dyr=ye-ys;
dxr=dyr/dy*dx;
npr=nye-nys;
%
plot(s(:,1),s(:,2),s(nys:nys,1),s(nys:nys,2),tp,peak,'o')
title(['Risetime is ',num2str(dxr),' with ',num2str(npr),'points'])
```

Distribution

Admnstr
Defns Techl Info Ctr
Attn DTIC-OCF
8725 John J Kingman Rd Ste 0944
FT Belvoir VA 22060-6218

Ofc of the Dir Rsrch and Engrg
Attn R Menz
Pentagon Rm 3E1089
Washington DC 20301-3080

Ofc of the Secy of Defns
Attn ODDRE (R&AT) G Singley
Attn ODDRE (R&AT) S Gontarek
The Pentagon
Washington DC 20301-3080

OSD
Attn OUSD(A&T)/ODDDR&E(R) R Tru
Washington DC 20301-7100

CECOM
Attn PM GPS COL S Young
FT Monmouth NJ 07703

CECOM RDEC Elect System Div Dir
Attn J Niemela
FT Monmouth NJ 07703

CECOM
Sp & Terrestrial Commctn Div
Attn AMSEL-RD-ST-MC-M H Soicher
FT Monmouth NJ 07703-5203

Dir of Assessment and Eval
Attn SARD-ZD H K Fallin Jr
103 Army Pentagon Rm 2E673
Washington DC 20301-0163

Hdqtrs Dept of the Army
Attn DAMO-FDT D Schmidt
400 Army Pentagon Rm 3C514
Washington DC 20301-0460

MICOM RDEC
Attn AMSMI-RD W C McCorkle
Redstone Arsenal AL 35898-5240

US Army Avn Rsrch, Dev, & Engrg Ctr
Attn T L House
4300 Goodfellow Blvd
St Louis MO 63120-1798

US Army CECOM Rsrch, Dev, & Engrg Ctr
Attn R F Giordano
FT Monmouth NJ 07703-5201

US Army Edgewood Rsrch, Dev, & Engrg Ctr
Attn SCBRD-TD J Vervier
Aberdeen Proving Ground MD 21010-5423

US Army Info Sys Engrg Cmnd
Attn ASQB-OTD F Jenia
FT Huachuca AZ 85613-5300

US Army Materiel Sys Analysis Agency
Attn AMXSJ-D J McCarthy
Aberdeen Proving Ground MD 21005-5071

US Army Matl Cmnd
Dpty CG for RDE Hdqtrs
Attn AMCRD BG Beauchamp
5001 Eisenhower Ave
Alexandria VA 22333-0001

US Army Matl Cmnd
Prin Dpty for Acquisition Hdqtrs
Attn AMCDCG-A D Adams
5001 Eisenhower Ave
Alexandria VA 22333-0001

US Army Matl Cmnd
Prin Dpty for Techlgy Hdqtrs
Attn AMCDCG-T M Fisette
5001 Eisenhower Ave
Alexandria VA 22333-0001

US Army Natick Rsrch, Dev, & Engrg Ctr
Acting Techl Dir
Attn SSCNC-T P Brandler
Natick MA 01760-5002

US Army Rsrch Ofc
Attn G Iafrate
4300 S Miami Blvd
Research Triangle Park NC 27709

Distribution

US Army Simulation, Train, & Instrmntn
Cmnd
Attn J Stahl
12350 Research Parkway
Orlando FL 32826-3726

US Army Tank-Automtv & Armaments Cmnd
Attn AMSTA-AR-TD C Spinelli
Bldg 1
Picatinny Arsenal NJ 07806-5000

US Army Tank-Automtv Cmnd Rsrch, Dev, &
Engrg Ctr
Attn AMSTA-TA J Chapin
Warren MI 48397-5000

US Army Test & Eval Cmnd
Attn R G Pollard III
Aberdeen Proving Ground MD 21005-5055

US Army Train & Doctrine Cmnd
Battle Lab Integration & Techl Dirctr
Attn ATCD-B J A Klevecz
FT Monroe VA 23651-5850

US Military Academy
Dept of Mathematical Sci
Attn MAJ D Engen
West Point NY 10996

USAASA
Attn MOAS-AI W Parron
9325 Gunston Rd Ste N319
FT Belvoir VA 22060-5582

Nav Surface Warfare Ctr
Attn Code B07 J Pennella
17320 Dahlgren Rd Bldg 1470 Rm 1101
Dahlgren VA 22448-5100

GPS Joint Prog Ofc Dir
Attn COL J Clay
2435 Vela Way Ste 1613
Los Angeles AFB CA 90245-5500

DARPA
Attn B Kaspar
Attn L Stotts
3701 N Fairfax Dr
Arlington VA 22203-1714

ARL Electromag Group
Attn Campus Mail Code F0250 A Tucker
University of Texas
Austin TX 78712

Dir for MANPRINT
Ofc of the Deputy Chief of Staff for Prsnrl
Attn J Hiller
The Pentagon Rm 2C733
Washington DC 20301-0300

US Army Rsrch Lab
Attn AMSRL-CI-LL Techl Lib (3 copies)
Attn AMSRL-CS-AL-TA Mail & Records
Mgmt
Attn AMSRL-CS-AL-TP Techl Pub (3 copies)
Attn AMSRL-SE-DE C Reiff (5 copies)
Attn AMSRL-SE-DE J Miletta
Attn AMSRL-SE-DP M Litz
Attn AMSRL-SE-DS L Jasper
Attn AMSRL-SE-DS W O Coburn
Adelphi MD 20783-1197

REPORT DOCUMENTATION PAGE			<i>Form Approved OMB No. 0704-0188</i>	
Public reporting burden for this collection of information is estimated to average 1 hour per response, including the time for reviewing instructions, searching existing data sources, gathering and maintaining the data needed, and completing and reviewing the collection of information. Send comments regarding this burden estimate or any other aspect of this collection of information, including suggestions for reducing this burden, to Washington Headquarters Services, Directorate for Information Operations and Reports, 1215 Jefferson Davis Highway, Suite 1204, Arlington, VA 22202-4302, and to the Office of Management and Budget, Paperwork Reduction Project (0704-0188), Washington, DC 20503.				
1. AGENCY USE ONLY (Leave blank)		2. REPORT DATE March 1998	3. REPORT TYPE AND DATES COVERED Final, January to October 1997	
4. TITLE AND SUBTITLE An Amplified Broadband Dipole E-Dot Sensor			5. FUNDING NUMBERS PE: 62120A	
6. AUTHOR(S) Christian G. Reiff				
7. PERFORMING ORGANIZATION NAME(S) AND ADDRESS(ES) U.S. Army Research Laboratory Attn: AMSRL-SE-DS (creiff@arl.mil) 2800 Powder Mill Road Adelphi, MD 20783-1197			8. PERFORMING ORGANIZATION REPORT NUMBER ARL-TR-1613	
9. SPONSORING/MONITORING AGENCY NAME(S) AND ADDRESS(ES) U.S. Army Research Laboratory 2800 Powder Mill Road Adelphi, MD 20783-1197			10. SPONSORING/MONITORING AGENCY REPORT NUMBER	
11. SUPPLEMENTARY NOTES AMS code: 622120.140 ARL PR: 7NEYW3				
12a. DISTRIBUTION/AVAILABILITY STATEMENT Approved for public release; distribution unlimited.			12b. DISTRIBUTION CODE	
13. ABSTRACT (Maximum 200 words) <p>This report describes the incorporation of an amplifier in a dipole sensor. The entire package is contained in a semirigid coaxial cable end. This configuration provides a flat E-dot field response from dc to 2 GHz. The amplification of the sensor response before cable losses allows the correction for the losses by convolution in the frequency domain. The MATLAB algorithms used to correct measurement system losses are described.</p>				
14. SUBJECT TERMS Electric field sensor, amplifier, convolved signal processing			15. NUMBER OF PAGES 40	
			16. PRICE CODE	
17. SECURITY CLASSIFICATION OF REPORT Unclassified	18. SECURITY CLASSIFICATION OF THIS PAGE Unclassified	19. SECURITY CLASSIFICATION OF ABSTRACT Unclassified	20. LIMITATION OF ABSTRACT UL	